

Experimental and numerical studies on damage and failure behavior of anisotropic ductile metals

Sanjeev Koirala^{1,*}, Steffen Gerke¹, and Michael Brünig¹

¹ Institut für Mechanik und Statik, Universität der Bundeswehr München, Werner-Heisenberg-Weg 39, 85579 Neubiberg, Germany

The paper deals with experiments and numerical simulations of the biaxially loaded H-specimen to study the damage and failure in anisotropic ductile metals. The deformation and failure behavior of anisotropic ductile metals depend both on load ratio and loading direction with respect to the rolling direction. Experiments focusing on shear-compression stress states have been performed and digital image correlation (DIC) is used to monitor the strain fields. Numerical simulations based on the Hill48 anisotropic yield criterion are used to predict the stress states of the investigated anisotropic aluminum alloy EN AW-2017A. The fractured surfaces are visualized by scanning electron microscopy (SEM). The experimental-numerical technique clearly shows the influence of loading direction and the stress state on the evolution of damage processes.

© 2023 The Authors. *Proceedings in Applied Mathematics & Mechanics* published by Wiley-VCH GmbH.

1 Introduction

It is well known that plastic anisotropy in rolled metal sheets is due to the different forming processes, like deep drawing or rolling. Furthermore, they undergo through various stress states. This induced plastic anisotropy and different stress states have influences on the damage and fracture processes. Therefore, it is important to take these induced anisotropic effects in constitutive models to capture the mechanical behavior of the material more accurately. The very first quadratic anisotropic yield criterion developed by Hill48 [1] is anisotropic generalisation of the isotropic yield criteria proposed by von Mises. Although, the calibration of the material parameters is relatively simple, in some cases both r -value (ratio of plastic strain increments in width and thickness direction) and yield stresses were not accurately predicted. Since then many anisotropic constitutive models have been developed [2, 3]. These non-quadratic yield criterion are more accurate but the calibration of the material parameters require more and different type of experiments.

Generally, unnotched tensile specimens are used to determine the elastic-plastic material parameters as well as to study the influence of stress state on damage and fracture processes. Also, specially designed shear specimens have been used to investigate the damage and fracture behavior [4, 5]. However, only small range of stress triaxialities (ratio of mean stress to equivalent stress) are covered by these experiments. Thus, newly designed specimens were proposed [6] to study the damage and fracture at wide range of stress states. Furthermore, anisotropies and their effect in damage and fracture processes have to be taken into account. In this paper, experiments with new biaxially loaded H-specimen have been carried out to analyze the influence of shear combined with compression loading and material orientation on the damage and fracture of the anisotropic aluminum. DIC is used to capture the strain fields in the critical areas of the specimen. The fractured surfaces are analysed with the help of SEM which reveals useful informations on various damage and fracture processes at the micro-level.

2 Constitutive model

The Hill48 yield criterion [1] (assuming plane stress conditions) is used to characterize the anisotropic plastic behavior and is given as

$$f^{pl} = \sqrt{\frac{1}{2}[(G + H)\sigma_x^2 - 2H\sigma_x\sigma_y + (F + H)\sigma_y^2 + 2N\sigma_{xy}^2]} - \bar{\sigma} = 0 \quad (1)$$

where G , H , F and N are the anisotropic material parameters and $\bar{\sigma}$ is the equivalent yield stress. These parameters are determined from uniaxial tensile tests which will be discussed in the next section. Associated flow rule is used to describe the evolution of the plastic strains

$$\dot{\epsilon}_{ij}^{pl} = \dot{\lambda} \frac{\partial f^{pl}}{\partial \sigma_{ij}} \quad (2)$$

where $\dot{\lambda}$ is a scalar parameter characterizing the amount of plastic strain increments. Stress triaxiality taking material anisotropy into account is defined as

$$\eta = \frac{\sigma_m}{\sigma_{eq}} = \frac{I_1}{3\sqrt{\frac{1}{2}[(G + H)\sigma_x^2 - 2H\sigma_x\sigma_y + (F + H)\sigma_y^2 + 2N\sigma_{xy}^2]}} \quad (3)$$

* Corresponding author: e-mail sanjeev.koirala@unibw.de, phone +49 89 6004 2905

This is an open access article under the terms of the Creative Commons Attribution-NonCommercial-NoDerivs License, which permits use and distribution in any medium, provided the original work is properly cited, the use is non-commercial and no modifications or adaptations are made.

where σ_m is the mean stress, σ_{eq} is the equivalent stress based on the Hill yield criterion (eq.1) and I_1 is the first stress invariant. η is a significant parameter to identify ductile damage processes. For example, the value of η is generally higher for tension dominated loading (around 0.33 – 1) which indicates that the damage is mainly due to void growth and their coalescence. On the other hand, for η (around 0 – 0.33) the damage process is due to micro-shear-cracks.

3 Material and parameter identification

The material investigated is aluminium alloy (EN AW-2017A) which is extensively used in automotive and aircraft application. The chemical composition is shown in Tab.1.

Table 1: Chemical composition of EN AW-2017A aluminum alloy (% weight)

Material	Cu	Fe	Mn	Mg	Si	Zn	Cr	Others	Al
EN AW-2017A	4.0	0.7	0.7	0.7	0.5	0.25	0.10	0.15	to balance

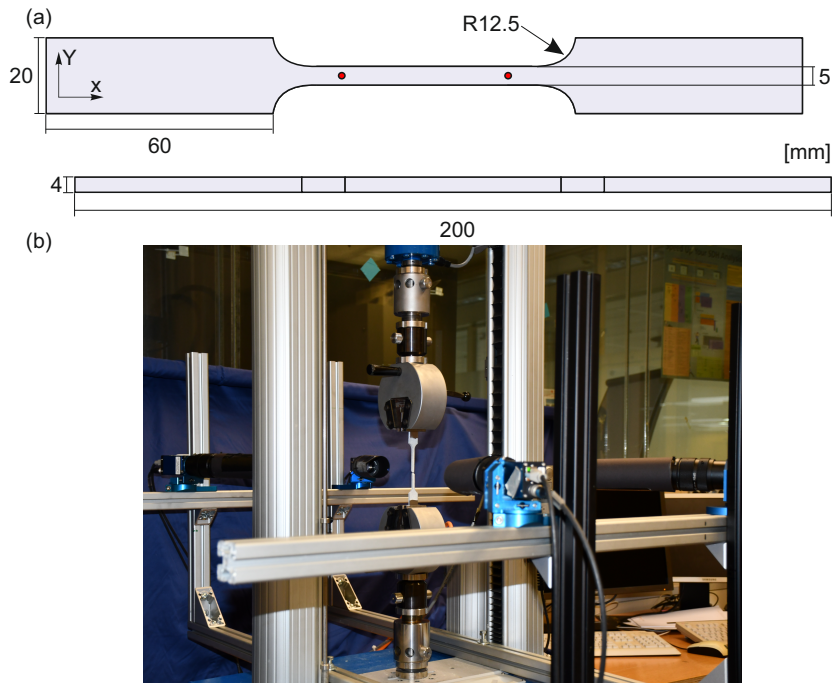


Fig. 1: Geometry of the tensile specimen (a) and uniaxial tests experimental setup (b)

The classical dog-bone-shaped tensile specimens as shown in Fig. 1(a) are cut from 4mm thick sheets and in three different rolling directions namely parallel to the rolling direction (RD), 45° to the RD (DD) and 90° to the RD (TD). Then, uniaxial tensile tests are conducted in uniaxial test machine type inspekt Table 50-1 (produced by Hegewal and Peschke, Nossen, Germany) shown in Fig. 1(b). DIC is used to analyze the three-dimensional displacement and strain fields of the surfaces of the specimen. Four cameras (each pair on front and back surface of the specimen) are calibrated to a common coordinate system using the double sided calibration target. Displacements of the two red points (red points in Fig. 1(a)) are read and their relative displacement in x-direction is calculated as $\Delta u_{ref} = \Delta u_1 - \Delta u_2$. Fig. 2(b) shows the experimentally obtained and numerically fitted flow curves for RD, DD and TD. These curves are fitted using Voce law [7]

$$\bar{\sigma} = \bar{\sigma}_0 + R_0 \epsilon^{pl} + R_\infty (1 - e^{-b \epsilon^{pl}}) \quad (4)$$

with the initial yield stress $\bar{\sigma}_0$, the hardening moduli R_∞ and R_0 , the equivalent plastic strain ϵ_{pl} and the hardening exponent b . The obtained parameters are shown in Tab.2.

One of the widely used plastic anisotropy quantity in sheet metals is known as Lankford coefficient (also called r -value). The Lankford coefficient is given by

$$r = \frac{\dot{\epsilon}_y^{pl}}{\dot{\epsilon}_z^{pl}} \quad (5)$$

Table 2: Plastic material parameters

	$\bar{\sigma}_0$ [MPa]	R_o [MPa]	R_∞ [MPa]	b
RD	313	464	147	20
DD	297	474	127	28
TD	308	445	128	25

where $\dot{\epsilon}_y^{pl}$ and $\dot{\epsilon}_z^{pl}$ are plastic strain increments in width and through thickness directions, respectively. Assuming that the volume remains constant during the plastic deformation, the plastic strain increment in thickness direction is given by

$$\dot{\epsilon}_z^{pl} = -(\dot{\epsilon}_x^{pl} + \dot{\epsilon}_y^{pl}) \quad (6)$$

With the help of the measured strains on the surface of the specimen, evolution of r -value is plotted in Fig. 2(a). Then, it is fitted with a straight line between 5% – 20% of plastic equivalent strain for loading in RD, DD and TD. Another way of fitting r -value is to use a linear equation as in [8] where it is not constant during the experiment and is continuously evolving during the plastic deformation. But in this work only the constant r -value is taken and the fitted curve seems to be in good agreement with experimental results within the specified strain range. The determined r -values are represented in Tab.3. Furthermore, there are various ways to calculate the anisotropic material parameters in Hill48 plasticity model (eq.1) as mentioned in [9]. In [10], they have used the combined method i.e. both the yield stresses and r -values from the tensile tests in different rolling directions are utilized to determine the anisotropic material parameters. In this paper the material parameters are calculated only using r -value in RD, DD and TD, which leads to

$$G = \frac{2}{1 + r_0} \quad (7)$$

$$H = 2 - G \quad (8)$$

$$F = \frac{H}{r_{90}} \text{ and } N = (r_{45} + \frac{1}{2})(F + G) \quad (9)$$

Based on these equations G , H , F and N are calculated and shown in Tab.4.

Table 3: Lankford coefficients

r_0	r_{45}	r_{90}
0.597	0.783	0.695

Table 4: Anisotropic material parameters

G	H	F	N
1.252	0.748	1.076	2.986

4 Experimental and numerical results

The biaxial experiments with H-specimen are performed on the biaxial test machine LFM-BIAX 20 kN produced by Walter+Bai, Switzerland. It has four individually driven electro-mechanical cylinders with ± 20 kN maximum load. The specimen is clamped in the four heads as shown in Fig. 3. During the experiments, DIC system is used to monitor the strain fields on the surfaces of critical regions of the specimens where inelastic deformations tend to localize. Two 6MPx cameras with 75mm lenses are installed to achieve DIC system in stereo setup. In this paper the experimental technique is only briefly summarized. For the detail description please refer to [11].

As shown in Fig. 4, the H-specimen is simultaneously loaded in two perpendicular axes by forces F_1 and F_2 . The loads are applied in two axes keeping the loading ratio $F_1/F_2 = 1/ - 0.5$ throughout the experiment. In this way, in the notches of

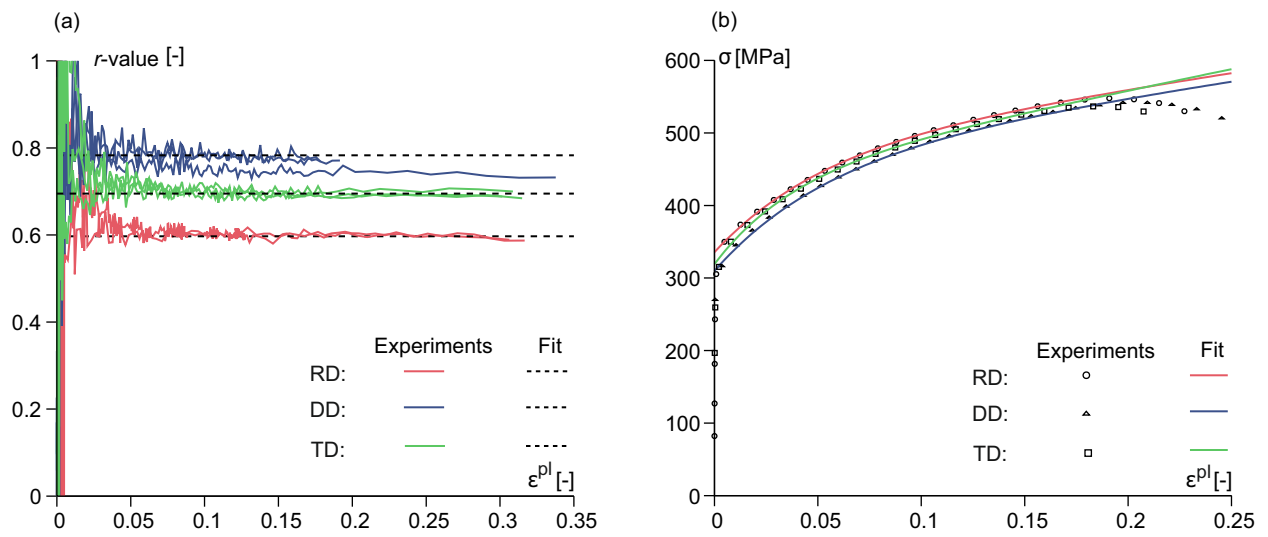


Fig. 2: r -value versus equivalent plastic strain (ϵ_{pl}) (a) and true stress versus ϵ_{pl} (b)

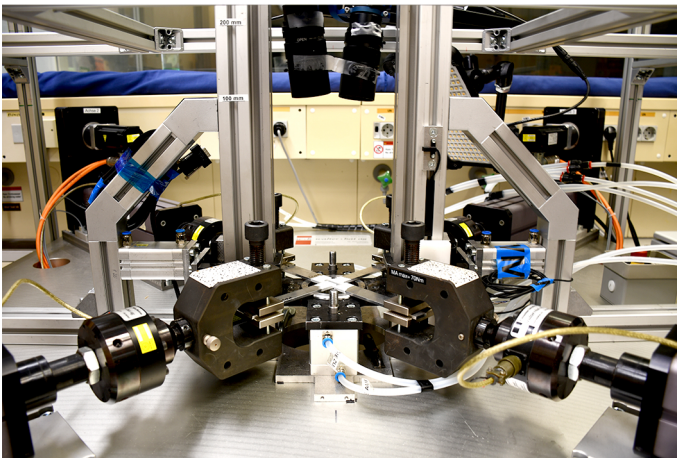


Fig. 3: Biaxial test machine

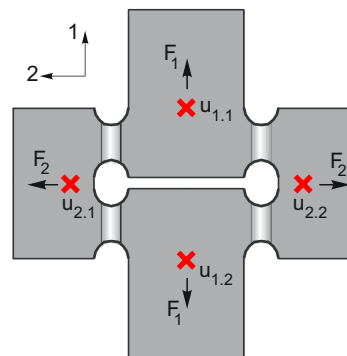


Fig. 4: Forces and displacements of the H-specimen

the specimen, shear loading is superimposed with compression. The tests are performed three times for each rolling directions (RD, DD and TD). Hence, the analysis of the effect of material anisotropy with multi-axial loading can be realised. The relative displacements (displacements of red points) in axis 1 and axis 2 are given by $\Delta u_{ref,1} = \Delta u_{1,1} - \Delta u_{1,2}$ and $\Delta u_{ref,2} = \Delta u_{2,1} - \Delta u_{2,2}$ respectively. Experimental and numerically simulated load-displacement curves for load ratio $F_1/F_2 = 1/-0.5$ is shown in Fig. 5(a). Like for other load ratios [12], small differences could be seen between loading in RD, DD and TD. The maximum load for loading in RD and TD in axis 1 is almost same and is around $F_1 = 7.26$ kN, but for loading in DD it is only $F_1 = 7.11$ kN. Similarly, the displacement at the onset of fracture for DD in axis 1 is $\Delta u_{ref,1} = 1.92$ mm, whereas for RD and TD it is equal to $\Delta u_{ref,1} = 1.80$ mm and $\Delta u_{ref,1} = 1.82$ mm respectively. These differences show that the behavior is little more ductile for loading in DD as compared to loading in RD and TD.

Fig. 5(b) indicates the first principal strain distribution in the notch of the specimen shortly before the fracture. The black lines in the figure show the rolling directions. The principal strain bands for all directions are small and are diagonally oriented and for loading in DD it attains the maximum value of 43 % when compared to loading in RD and TD. Furthermore, the distribution of stress triaxiality in the cross-section of the notches after elastic-plastic numerical simulations are depicted in Fig. 6(b). The stress triaxiality value is in the range of 0 and -0.15 which is typical for shear combined with compression loading. In addition, the evolution of average value of stress triaxiality ($\bar{\eta}$) over the notched cross-section for RD, DD and TD is shown in Fig. 6(a). $\bar{\eta}$ is slightly lower for loading in DD than loading in RD and TD. But, overall $\bar{\eta}$ during the whole loading process is only slightly changed for all rolling directions. Hence, the H-specimen is quite suitable to study the damage and failure behavior of anisotropic ductile metals in negative triaxiality region.

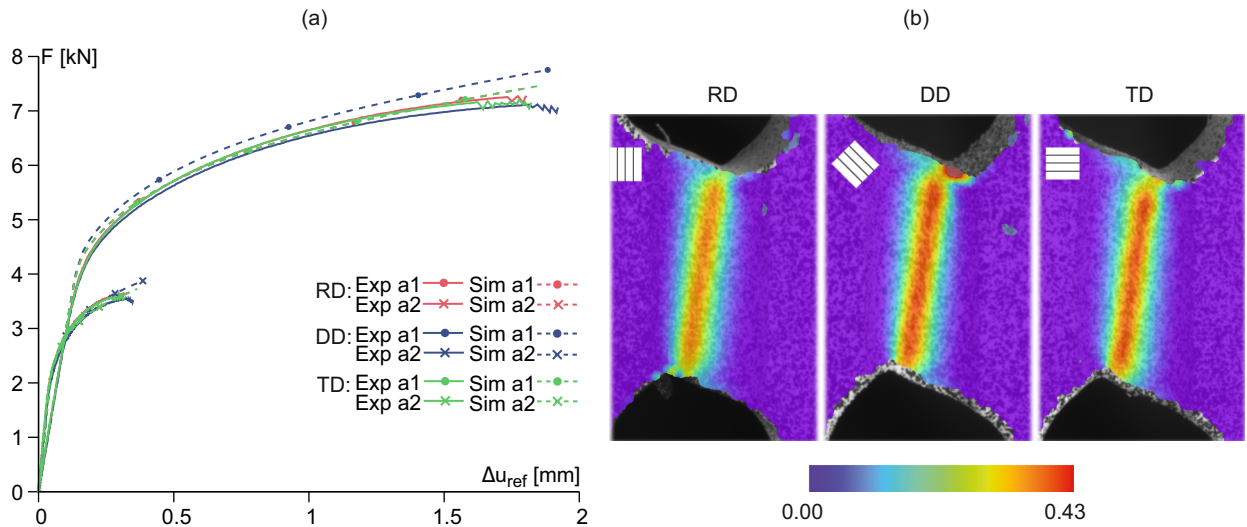


Fig. 5: Load-displacement curves (a) and distribution of first principal strain (b) for the load ratio $F_1/F_2 = 1/ - 0.5$

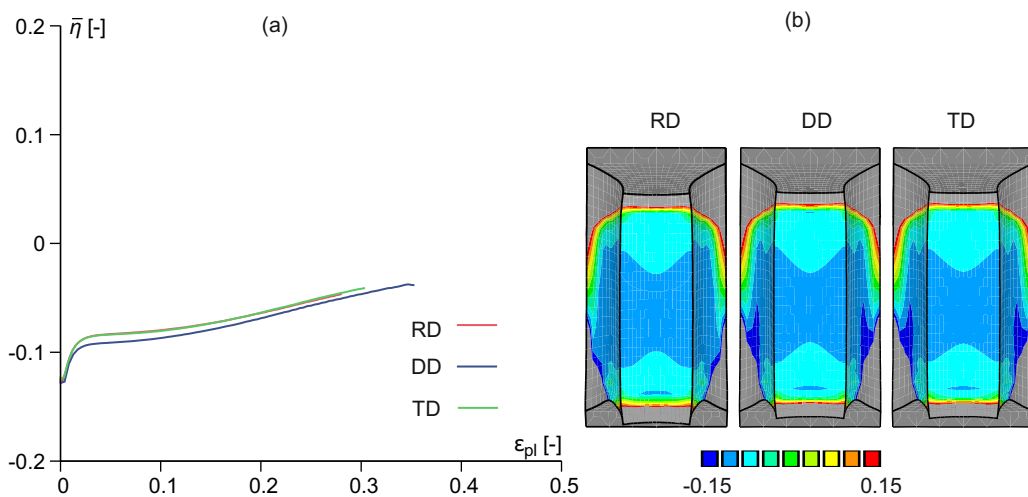


Fig. 6: Average stress triaxiality $\bar{\eta}$ versus the equivalent plastic strain ϵ_{pl} (a) and the distribution of stress triaxiality (b) for the load ratio $F_1/F_2 = 1/ - 0.5$

The cross section of fractured notches were examined by SEM and the pictures are arranged in Fig. 7. For loading in RD and TD the voids are slightly bigger as compared to DD. Furthermore, they are sheared and superimposed by micro-shear-cracks leading to shear fracture. Again, the damage and fracture also depend on loading in different directions for the investigated anisotropic material.

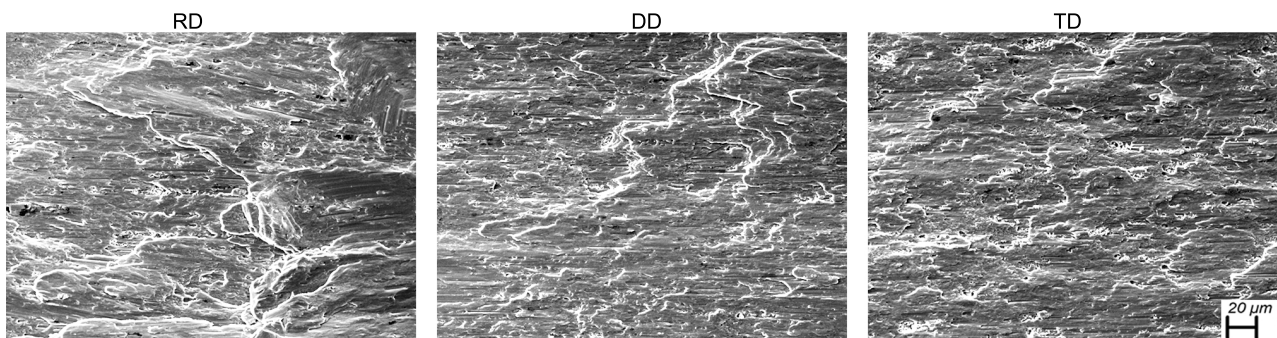


Fig. 7: SEM pictures for the load ratio $F_1/F_2 = 1/ - 0.5$

5 Conclusions

The effect of the load ratios and loading directions on damage and fracture behavior of the anisotropic aluminum alloy EN AW 2017A using biaxially loaded H-specimen has been thoroughly investigated. Specimens loaded in DD show higher ductility as compared to loading in RD and TD. Also, the obtained results show that the orientation of the specimen with respect to the principal axes of anisotropy has demonstrable influence on damage and fracture processes on micro-level. These results will be used to model the damage and failure in anisotropic ductile metals.

Acknowledgements This research was funded by the Deutsche Forschungsgemeinschaft (DFG, German Research Foundation) - Project number 394286626. This financial support is gratefully acknowledged. Open access funding enabled and organized by Projekt DEAL.

References

- [1] R. Hill, A theory of the yielding and plastic flow of anisotropic metals, *Proc. R. Soc. Lond* **193**, 281 – 297 (1948).
- [2] F. Barlat, H. Aretz, J.W. Yoon, M.E. Karabin, J.C. Brem, R.E. Dick, Linear transformation-based anisotropic yield functions, *International Journal of Plasticity* **21**, 1009-1039 (2005).
- [3] F. Bron, J. Besson, A yield function for anisotropic materials - application to aluminum alloys, *International Journal of Plasticity* **20**, 937-963 (2004).
- [4] X. Gao, G. Zhang, C. Roe, A study on the effect of the stress state on ductile fracture. *International Journal of Damage Mechanics* **19**, 75-94 (2010).
- [5] Q. Yin, C. Soyarslan, K. Isik, A.E. Tekkaya, A grooved in-plane torsion test for the investigation of shear fracture in sheet materials. *International Journal of Solids and Structures* **66**, 121-132 (2015).
- [6] S. Gerke, P. Adulyasak and M. Brünig, New biaxially loaded specimens for the analysis of damage and fracture in sheet metals, *International Journal of Solids and Structures* **110**, 209 – 218 (2017).
- [7] E. Voce, A practical strain-hardening function, *Metallurgia* **51**, 219-226 (1955).
- [8] J. Lian, F. Shen, X. Jia, D. Ahn, D. Chae, S. Münstermann, W. Bleck, An evolving non-associated Hill48 plasticity model accounting for anisotropic hardening and r-value evolution and its application to forming limit prediction, *International Journal of Solids and Structures* **151**, 20-44 (2018).
- [9] A. Holger, Numerical analysis of diffuse and localized necking in orthotropic sheet metals, *International Journal of Plasticity* **23**, 798-840 (2007).
- [10] M. Brünig, S. Gerke and S. Koirala, Biaxial experiments and numerical analysis on stress-state-dependent damage and failure behavior of the anisotropic aluminium alloy EN AW-2017A, *Metals* **11**, 1214 (2021).
- [11] M. Brünig, M. Zistl and M. Gerke, Numerical analysis of experiments on damage and fracture behavior of differently preloaded aluminium alloy specimens, *Metals* **11**, 381 (2021).
- [12] M. Brünig, S. Koirala and S. Gerke, Analysis of damage and failure in anisotropic ductile metals based on biaxial experiments with the H-specimen, *Experimental Mechanics* **62**, 183-197 (2022).